EUSIPCO 2013 1569742623

REDUCING THE COMPUTATIONAL COMPLEXITY OF RECONSTRUCTION IN COMPRESSED SENSING NONUNIFORM SAMPLING

Ruben Grigoryan, Tobias Lindstrøm Jensen, Thomas Arildsen and Torben Larsen

{rug, tlj, tha, tl}@es.aau.dk
Department of Electronic Systems, Aalborg University

ABSTRACT

This paper proposes a method that reduces the computational complexity of signal reconstruction in single-channel nonuniform sampling while acquiring frequency sparse multi-band signals. Generally, this compressed sensing based signal acquisition allows a decrease in the sampling rate of frequency sparse signals, but requires computationally expensive reconstruction algorithms. This can be an obstacle for real-time applications. The reduction of complexity is achieved by applying a multi-coset sampling procedure. This proposed method reduces the size of the dictionary matrix, the size of the measurement matrix and the number of iterations of the reconstruction algorithm in comparison to the direct single-channel approach. We consider an orthogonal matching pursuit reconstruction algorithm for single-channel sampling and its modification for multi-coset sampling. Theoretical as well as numerical analyses demonstrate order of magnitude reduction in execution time for typical problem sizes without degradation of the signal reconstruction quality.

Index Terms— compressed sensing, multi-coset sampling, nonuniform sampling, reconstruction algorithm

1. INTRODUCTION

Signals generally must be sampled at the Nyquist rate, otherwise aliasing will prevent correct reconstruction of the signal. However, if we narrow the scope of signals to frequency sparse signals, we can successfully apply sub-Nyquist rate sampling [1, 2]. This type of signal acquisition assumes that the number of the obtained samples (measurements) is lower than the number of Nyquist rate samples. Frequency sparsity implies that the energy of a signal is concentrated in small joint or disjoint parts (i.e. bands or individual tones) of the spectrum. If sub-Nyquist rate sampling is possible, then cheaper analog front ends may be used, or signal acquisition can be accelerated. Sub-Nyquist sampling has evolved from bandpass sampling to various compressed sensing (CS) architectures such as the random demodulator [3], the nonuniform sampler [4], the multi-coset sampler [2, 5, 6] and the modulated wideband converter [7].

The key idea of CS is to use advanced reconstruction procedures to compensate for the lack of measurements. In the language of linear algebra, the process of the CS signal reconstruction is the process of solving an under-determined linear system with fewer equations than unknowns. The concept of sparsity is used to establish the rules under which a unique signal reconstruction is possible [8]. By contrast to CS, traditional Nyquist rate sampling corresponds to a system with the isometric matrix that can be easily solved.

An obstacle for real-time CS applications is the high complexity of reconstruction [4]. Therefore, it is important to find ways to reduce the computational costs of signal recovery. There are two main groups of reconstruction algorithms [9]: 1) greedy algorithms which find the dominant components of the solution; and 2) relaxation methods which solve convex (such as ℓ_1-minimization) and non-convex problems.

In this paper, we propose a method that reduces computational complexity of signal reconstruction in single-channel nonuniform sampling (SC-NUS). SC-NUS is one of the CS approaches that can be used for acquisition of frequency sparse signals. SC-NUS selects samples from a Nyquist grid and uses them to recover the whole Discrete Fourier Transform (DFT) of the Nyquist rate samples. Frequency sparse signals that can be acquired with SC-NUS may have both individual tones and bands. However, in some applications such as telecommunications, the energy of a signal is concentrated in a small number of bands rather than in a large number of independent tones. In this case, a multi-coset sampler (MCS) architecture is beneficial [2, 5, 6]. MCS also selects samples from a Nyquist grid, but does it periodically. Assume that a real-valued multi-band signal has to be sensed with SC-NUS with the predefined undersampling ratio. That can be done in two ways: 1) in the direct SC-NUS manner; and 2) in the MCS manner. We show that the computational complexity of the signal reconstruction in MCS is lower than in direct SC-NUS. This reduction of complexity is the result of two factors. First, the size of the measurement and the dictionary matrices in MCS is smaller than the size of the corresponding matrices in SC-NUS. Secondly, the number of iterations performed by the reconstruction algorithms in MCS is lower than the number of iterations in SC-NUS reconstruction. On the whole, we reduce the number of arithmetical operations

that are performed at the reconstruction stage. Numerical simulations show that this reduction of computational complexity does not decrease the reconstruction quality. In this paper, we consider the Orthogonal Matching Pursuit (OMP) algorithm for SC-NUS and its modification for MCS. A noise free scenario is assumed for simplicity, but the method can also be applied to the noisy case.

A related method is presented in [4], where the authors propose to jointly reconstruct a set of sequentially sampled signals. However, this method works well only if the positions of tones and bands do not change significantly. In [10], the authors pointed out that reconstruction in the modulated wideband converter requires fewer FLoating-point OPerations (FLOP) than reconstruction in the random demodulator. Our proposed method extends this observation.

The outline of the paper is as follows. In Section 2, we describe single-channel nonuniform and multi-coset sampling, and present the main idea of the paper. Analytical and simulation results are shown in Section 3. We conclude the paper in Section 4.

2. SAMPLING SCHEMES

2.1. Single-channel nonuniform sampling

SC-NUS acquires only some of the Nyquist rate samples. In the reconstruction procedure, these measurements are used to recover the DFT of samples as they would be acquired at the full Nyquist rate. Therefore, we decrease the average sampling rate below the Nyquist rate. The process of sampling is illustrated in Fig. 1(a). In total, there are $N = 14$ Nyquist rate samples, and only $M = 8$ of them are acquired by SC-NUS. The so-called sampling pattern Λ defines which samples are obtained. In SC-NUS, the relation between the measurements and the unknown DFT is

$$\mathbf{y} = \mathbf{A}\cdot\mathbf{x} = \mathbf{D}\cdot\mathbf{F}_N\cdot\mathbf{x}; \tag{1}$$

where $\mathbf{y} \in \mathbb{R}^{M\times 1}$ is a vector of the acquired samples, $\mathbf{D} \in \mathbb{Z}^{M\times N}$ is the decimation (measurement) matrix that corresponds to the sampling pattern, $\mathbf{F}_N \in \mathbb{C}^{N\times N}$ is the DFT (dictionary) matrix of order N, and $\mathbf{x} \in \mathbb{C}^{N\times 1}$ is the unknown DFT of the Nyquist rate samples. The vector $\mathbf{x}$ is assumed to be sparse with $K_1 < M$ non-zero elements. The support S is the set of indices of these non-zero elements.

The OMP algorithm [9] can be used to recover the unknown input signal in SC-NUS. A reconstruction with OMP is performed in two steps: 1) OMP finds the support S of $\mathbf{x}$ (see Algorithm 1); 2) the actual values of $\mathbf{x}$ in the support are obtained with the least squares method applied to $\mathbf{y} \approx \mathbf{A}^S\cdot\mathbf{x}_S$. The symbol S in the superscript and in the subscript denotes the column and the row restriction of the matrix and the vector, respectively. In Algorithm 1, we utilize the fact that real-valued signals have conjugate-symmetric DFT [6].

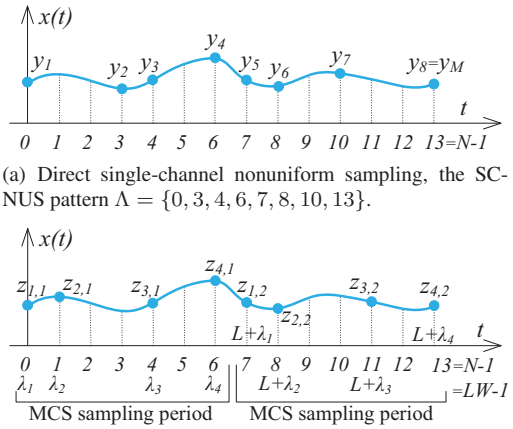

(a) Direct single-channel nonuniform sampling, the SC-NUS pattern $\Lambda = \{0, 3, 4, 6, 7, 8, 10, 13\}$.

(b) Multi-coset sampling, the MCS period $L = 7$, the number of MCS periods $W = 2$, the number of sampling channels $P = 4$, the MCS pattern $\Lambda = \{0, 1, 4, 6\}$.

Fig. 1. Illustration of SC-NUS and MCS, the Nyquist grid is marked with the dotted lines.

2.2. Multi-coset sampling

MCS also selects the Nyquist rate samples but does it periodically [2, 5, 6]. The principle behind MCS is to use several parallel uniform samplers. These samplers acquire signal's values at the same rate but with different time offsets. The offsets are defined by the MCS pattern $\Lambda = \{\lambda_1, \ldots, \lambda_P\} \subset \{0, 1, \ldots, L-1\}$. MCS can be seen as a time-interleaved sampler with P out of L channels. Accordingly, only P samples are selected from every bunch of L consecutive Nyquist-rate samples. L is called the MCS period. The process of MCS is illustrated in Fig. 1(b) where $W = 2$ MCS periods are shown. Denote by $z_{p,w} \in \mathbb{R}$, $p \in \{1, 2, \ldots, P\}, w \in \{1, 2, \ldots, W\}$ the wth output sample of the pth sampling channel. In discrete MCS, the relation between the measurements and the unknown DFT is described with the following equation [2, 5, 6]:

$$\mathbf{Y} = \mathbf{B}\cdot\mathbf{X} \tag{2}$$

where $\mathbf{Y} \in \mathbb{C}^{P\times W}$ is the known measurements,

$$\mathbf{Y} = \begin{pmatrix} \mathcal{F}_W([z_{1,1}\cdots z_{1,W}]^{\mathrm{T}}) \\ \vdots \\ \mathcal{F}_W([z_{P,1}\cdots z_{P,W}]^{\mathrm{T}}) \end{pmatrix} \circ \begin{pmatrix} \delta_{1,1} & \ldots & \delta_{1,W} \\ \vdots & \ddots & \vdots \\ \delta_{P,1} & \ldots & \delta_{P,W} \end{pmatrix} \tag{3}$$

$$\delta_{p,w} = \exp\left[\frac{-2\pi j\cdot\lambda_p\cdot(w-1)}{LW}\right], \tag{4}$$

the matrix $\mathbf{B} \in \mathbb{C}^{P\times L}$ is the known matrix that comprises both the measurement and the dictionary matrices. The elements of $\mathbf{B}$ are given by:

$$B_{p,\ell} = \frac{1}{L\cdot T}\exp\left[j\frac{2\pi}{L}\cdot\lambda_p\cdot\ell\right] \tag{5}$$

Algorithm 1 Find the support S of $\mathbf{x}$ with OMP [9]

Input: $\mathbf{y} \in \mathbb{R}^{M\times 1}, \mathbf{A} \in \mathbb{C}^{M\times N}, K_1 \in \mathbb{N}$
Output: $S \in \mathbb{N}_1^{K_1}$
1: $S \leftarrow \emptyset$, $\mathbf{r} \leftarrow \mathbf{y}$, $k \leftarrow 0$
2: **for** $k = 1$ to $\lceil K_1/2 \rceil$ **do**
3: $\quad i_{\max} \leftarrow \operatorname{argmax}_{i\in\{1,\dots,N\}\setminus S} \langle \mathbf{a}_i^*, \mathbf{r}\rangle$
4: $\quad i_{\text{sym}} \leftarrow N - i_{\max} + 1$
5: $\quad S \leftarrow S \cup \{i_{\max}, i_{\text{sym}}\}$
6: $\quad \mathbf{Q} \leftarrow$ Gram-Schmidt$(\mathbf{A}^S)$
7: $\quad \mathbf{r} \leftarrow \mathbf{r} - \mathbf{Q}\cdot\mathbf{Q}^*\cdot\mathbf{r}$
8: **end for**

and $\mathbf{X} \in \mathbb{C}^{L\times W}$ represents the unknown input signal, $p \in \{1, 2, \dots, P\}$, $w \in \{1, 2, \dots, W\}$, $\ell \in \{1, 2, \dots, L\}$. The matrix $\mathbf{X}$ is assumed to be sparse with $K_2 < P$ non-zero rows. In (3), $\mathcal{F}_W([\mathrm{z}_{p,1} \cdots \mathrm{z}_{p,W}]^{\mathrm{T}})$ is DFT of the samples obtained from the pth sampling channel, $\circ$ denotes the Hadamard product and $\delta_{p,w}$ represents the delay of the wth DFT bin in the pth sampling channel. The Nyquist sampling period T depends on the highest frequency component in the input signal. In total, the duration of the observed signal equals to LWT. Consider the matrix $\mathbf{X}$. If the unknown DFT of the input signal is sliced into L equal parts, then each row of $\mathbf{X}$ is one of these consecutive slices [2, 5, 6]. Signals with a few bands in the spectrum may result in a highly sparse $\mathbf{X}$.

Reconstruction with a greedy method for MCS is similar to the reconstruction for SC-NUS. We use the M-OMP algorithm that is the modification of OMP for multiple-measurement vectors problem [11]. M-OMP finds the support S, the indices of non-zero rows, of $\mathbf{X}$ (see Algorithm 2). Knowing the support, we can reconstruct the unknown signal with the least squares method similar to the SC-NUS case.

2.3. Multi-coset reconstruction in single-channel nonuniform sampling

Consider the sampling scenario where SC-NUS acquires multi-band signals. This can be done in two ways: 1) by the direct single-channel sampling that is described by (1); and 2) SC-NUS can select samples from the Nyquist grid in the same way as MCS. Therefore, SC-NUS can emulate MCS. In this case, the reconstruction problem (1) is replaced by (2).

The notable thing is that the reconstruction in MCS has lower computational complexity than the reconstruction in the direct SC-NUS. This reduction of the complexity is the result of two factors:

(1) in MCS, measurement and dictionary matrices are smaller than the corresponding matrices in SC-NUS; in other words, $\mathbf{A} \in \mathbb{C}^{M\times N}$ is replaced by $\mathbf{B} \in \mathbb{C}^{P\times L}$ where $P \ll M$ and $N \ll L$.

(2) in MCS reconstruction, the number of iterations performed by the reconstruction algorithm is lower than the number of iterations in the SC-NUS reconstruction. This happens due to the fact that usually $K_2 \ll K_1$.

Algorithm 2 Find the support S of $\mathbf{X}$ with M-OMP [11]

Input: $\mathbf{Y} \in \mathbb{C}^{P\times W}, \mathbf{B} \in \mathbb{C}^{P\times L}, K_2 \in \mathbb{N}_1$
Output: $S \in \mathbb{N}_1^{K_2}$
1: $S \leftarrow \emptyset$, $\mathbf{R} \leftarrow \mathbf{Y}$, $k \leftarrow 0$
2: **for** $k = 1$ to $\lceil K_2/2 \rceil$ **do**
3: $\quad i_{\max} \leftarrow \operatorname{argmax}_{i\in\{1,\dots,L\}\setminus S} \|\mathbf{b}_i^*\cdot\mathbf{R}\|_2^2$
4: $\quad i_{\text{sym}} \leftarrow L - i_{\max} + 1$
5: $\quad S \leftarrow S \cup \{i_{\max}, i_{\text{sym}}\}$
6: $\quad \mathbf{Q} \leftarrow$ Gram-Schmidt$(\mathbf{B}^S)$
7: $\quad \mathbf{R} \leftarrow \mathbf{R} - \mathbf{Q}\cdot\mathbf{Q}^*\cdot\mathbf{R}$
8: **end for**

The drawback of the proposed method is a decrease in the frequency support resolution. SC-NUS can reconstruct an individual DFT bin, whereas MCS can reconstruct only the whole frequency slice. This trade-off between the support resolution and the reconstruction complexity is out of the scope of the current paper and will be considered in our future research.

2.4. Complexity analysis

By computational complexity of a procedure we assume the number of FLOPs performed in this procedure, and by one FLOP we assume an arithmetic operation performed on two real floating-point numbers. Then, the complexity of the reconstruction in SC-NUS is

$$C^{\text{SC-NUS}} = C^{\text{SC-NUS}}_{\text{OMP}} + C^{\text{SC-NUS}}_{\text{Least Squares}}, \tag{6}$$

and the complexity of the MCS reconstruction is described with

$$C^{\text{MCS}} = C^{\text{MCS}}_{(3)} + C^{\text{MCS}}_{\text{M-OMP}} + C^{\text{MCS}}_{\text{Least Squares}}, \tag{7}$$

where $C^{\text{MCS}}_{(3)}$ denotes the complexity of the calculations (3). Assume that we use SC-NUS and MCS to recover the DFT of the Nyquist rate samples of a multi-band signal. The number of the samples is equal to $N = LW$ with $W \in \mathbb{N}_1$, SC-NUS and MCS are used with the same undersampling ratio $M/N = PW/(MW) = P/L$ and the frequency bands in a signal are aligned with the MCS frequency slices. We say that a band is aligned with a frequency slice if it occupies the whole slice (see Fig. 2). One MCS slice comprises W DFT bins. If F is the number of bands in the signal, then the number of non-zero elements of $\mathbf{x}$ in (1) is equal to $K_1 = 2FW$, where the factor 2 appears due to the symmetry of DFT. At the same time, F bands result only in $K_2 = 2F$ non-zero rows of the matrix $\mathbf{X}$ in (2). Knowing the values of M, N, P, L, W, K_1 and K_2, we can compute the complexity of the reconstruction in SC-NUS and MCS. For example, consider the complexity of the stage 3 in Algorithm 1 and Algorithm 2. For OMP, this number is

$$\begin{aligned} C^{\text{OMP}}_{\text{Stage 3}} &\simeq (8M - 2) \sum_{i=1}^{K_1/2} (N - 2(i-1)) \\ &\simeq 8PF(L - F + 1/W)W^3, \end{aligned} \tag{8}$$

and for M-OMP

$$C_{\text{Stage 3}}^{\text{M-OMP}} \simeq (8PW-2)\sum_{i=1}^{K_2/2}(L-2(i-1)) \simeq 8PF(L-F+1)W, \quad (9)$$

The ratio between these two numbers is

$$C_{\text{Stage 3}}^{\text{OMP}}/C_{\text{Stage 3}}^{\text{M-OMP}} \simeq W^2, \quad (10)$$

K_1 and K_2 are even due to the fact that we consider real-valued signals. So, for this stage, the reduction in complexity is the quadratic function of the number W. In MCS, the additional computations (3) have to be made prior to reconstruction. However, they have only $O(W\log(W))$ cost. On the whole, the direct counting shows that the MCS reconstruction requires fewer arithmetic operations than the SC-NUS reconstruction (see Section 3). This counting done using the code that computes the complexity according to (6) and (7). The parts of the code that calculate the costs of the standard operations, such as a matrix multiplication, a QR factorization and a backward substitution, are validated by comparison with the theoretical complexity available in the literature. The least squares solutions are obtained via QR factorization.

In (10), we assume that SC-NUS and MCS operates with the same undersampling ratio $M/N = P/L$. That is, we assume that the same sampling ratio results in the same reconstruction quality for both MCS and SC-NUS. We check this assumption with the numerical simulations.

3. NUMERICAL SIMULATIONS

The two analyzed signal acquisition methods were implemented and benchmarked in MATLAB.[1] In order to have a well defined number of arithmetic operations, a standard and naïve implementation of QR factorization and a least squares solver have been made [12]. Benchmarking is performed to make an overall numerical evaluation of the potential reconstruction speed-up in MCS compared to the direct SC-NUS.

3.1. Simulation setup

We consider simulation scenarios with multi-band frequency sparse signals. The signals are noise-free, real valued and generated in the time domain as N samples such that $N = LW$. The highest frequency component of a signal does not exceed $f_{\max}$. All bands in a signal have the same bandwidth, B. The average sampling rate f_{samp} is varied from $2f_{\max}/L$ to the Nyquist rate $f_{\text{Nyq}} = 2f_{\max}$ in steps of $2f_{\max}/L$. This shows how the reconstruction quality depends on the sampling rate. The reconstruction quality of one test signal is

[1]The source code is available online at http://www.sparsesampling.com/discretemulticoset/.

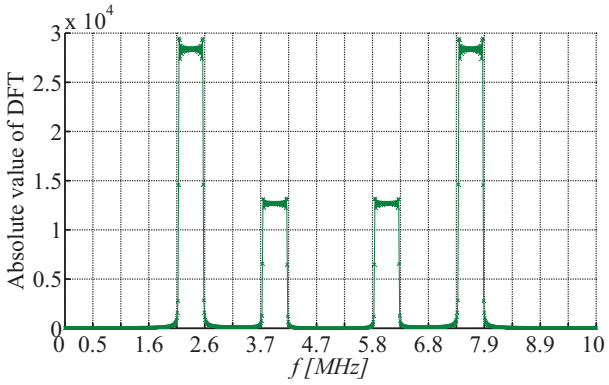

Fig. 2. Absolute DFT values versus frequency for an illustrative test signal with $F = 2$, $L = 19$, $N = 494$, $K_1 = 104$ and $K_2 = 4$. The vertical grid lines correspond to the MCS frequency slices.

measured with the relative root mean squared error:

$$E = \begin{cases} \sqrt{\|\widehat{\mathbf{x}} - \mathbf{x}\|_2^2/\|\mathbf{x}\|_2^2}, & \sqrt{\|\widehat{\mathbf{x}} - \mathbf{x}\|_2^2/\|\mathbf{x}\|_2^2} < 1 \\ 1, & \text{otherwise} \end{cases} \quad (11)$$

where $\mathbf{x}$ and $\widehat{\mathbf{x}}$ denote the original and recovered DFT coefficients, respectively. It is useless to consider the values of E greater than 1. Due to the possible spectrum leakage effect, the vector $\mathbf{x}$ is not completely sparse but rather compressible. Therefore, we cannot necessarily expect the error E to converge to zero in our simulations. An example of a test signal with $F = 2$ bands is illustrated in Fig. 2. The maximum frequency component is less than $f_{\max} = 5$ MHz and the Nyquist rate is $f_{\text{Nyq}} = 10$ MHz. The duration of the signal corresponds to $N = 494$ Nyquist rate samples which is 49.4 μs. The bands are placed randomly but always in the centers of the frequency slices. We choose L to be a prime number according to [9]; we use $L = 19$. The width of a frequency slice is thus $2f_{\max}/L \simeq 526$ kHz. The bandwidth of the individual bands of a test signal is set to $B = 486$ kHz. Such a bandwidth together with the spectrum leakage effect results in full occupation of the spectrum slice. The power of the individual bands are picked randomly over a dynamic range of 20 dB. It is assumed that the numbers K_1 and K_2 in Algorithm 1 and Algorithm 2 are known prior to the reconstruction of every signal. Otherwise, the performance of OMP and M-OMP are limited by methods chosen to evaluate the number of non-zero elements in the solution. This can distort the assessment. Simulations were performed for $F = \{1, \ldots, 6\}$ bands in the test signals. For every number of bands, we generate 1000 signal instances which was shown to ensure convergence of the results.

Selection of proper sampling patterns is itself a nontrivial problem. However, in case of noise free signals random sampling patterns work well for both SC-NUS and MCS [5]. The benchmarks were performed on a computer with an Intel X5670 2.93 GHz CPU running MATLAB R2012a.

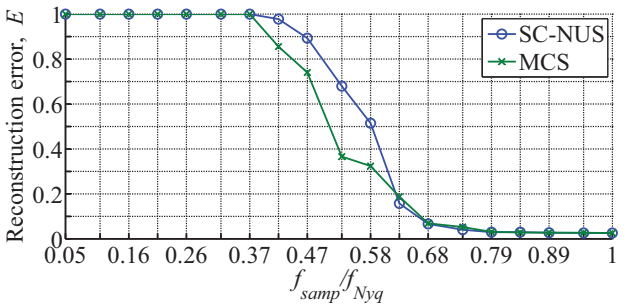

Fig. 3. Simulated average reconstruction error in SC-NUS and MCS versus average sampling rate. The number of bands is $F = 4$.

3.2. Reconstruction speed-up

As can be seen in Fig. 3, the proper reconstruction quality is achieved with the same sampling rate for both SC-NUS and MCS. By the proper quality, we mean the error-floor value of E resulting from spectrum leakage which does not depend on the sampling rate. This holds true for all F and ensures that the replacing SC-NUS by MCS does not degrade the recovery quality.

The theoretical and the benchmarked reconstruction speed-up are presented in Fig. 4. The benchmarked speed-up is the average value of the ratio of the benchmarked signal recovery time in SC-NUS to that in MCS. The theoretical speed-up is the ratio $C^{\text{SC-NUS}}/C^{\text{MCS}}$. As can be seen from the figure, the benchmarked speed-up is $4-7$ times lower than the theoretical speed-up. This can be explained by the fact that in the theoretical analysis, we disregard some practical issues such as the memory organization, the processor architecture and the cost of the auxiliary operations. Nevertheless, we do see the same behavior of the theoretical and benchmark speed-up.

4. CONCLUSIONS

This paper proposed a method that decreases the computational complexity of the reconstruction procedure in compressed sensing single-channel nonuniform sampling. We consider sampling of multi-band real-valued signals in noise free environment. The core idea of the proposed method is to use the multi-coset sampling approach. The drawback of the proposed method is the reduced frequency support resolution which may be acceptable in many applications. Depending on the number of bands in a signal, the number of arithmetic operations in the signal reconstruction stage is observed to decrease by the orders of magnitudes of 10^3 to 10^4. In addition, the proposed method does not degrade the reconstruction quality in the tested cases.

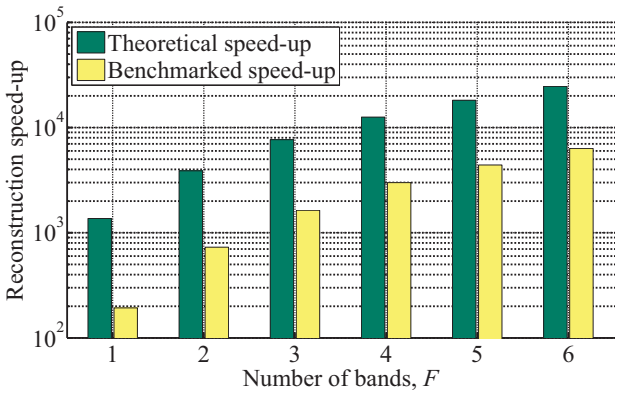

Fig. 4. Theoretical and benchmarked reconstruction speed-up versus number of bands, F.

5. REFERENCES

[1] R. Vaughan, N. Scott, and D. White, "The theory of bandpass sampling," *IEEE Trans. Signal Process.*, vol. 39, no. 9, pp. 1973–1984, Sep. 1991.

[2] P. Feng and Y. Bresler, "Spectrum-blind minimum-rate sampling and reconstruction of multiband signals," in *IEEE International Conference on Acoustics, Speech, and Signal Processing*, vol. 3, May 1996, pp. 1688–1691.

[3] J. Tropp, J. Laska, M. Duarte, J. Romberg, and R. Baraniuk, "Beyond Nyquist: Efficient sampling of sparse bandlimited signals," *IEEE Trans. Inf. Theory*, vol. 56, no. 1, pp. 520–544, Jan. 2010.

[4] M. Wakin, S. Becker, E. Nakamura, M. Grant, E. Sovero, D. Ching, J. Yoo, J. Romberg, A. Emami-Neyestanak, and E. Candès, "A nonuniform sampler for wideband spectrally-sparse environments," *IEEE J. Emerg. Sel. Topic Circuits Syst.*, vol. 2, no. 3, pp. 516–529, Sep. 2012.

[5] Y. Bresler, "Spectrum-blind sampling and compressive sensing for continuous-index signals," in *Information Theory and Applications Workshop*, Jan. 27 2008-Feb. 1 2008, pp. 547–554.

[6] M. Mishali and Y. C. Eldar, "Blind multiband signal reconstruction: Compressed sensing for analog signals," *IEEE Trans. Signal Process.*, vol. 57, no. 3, pp. 993–1009, 2009.

[7] M. Mishali, Y. Eldar, O. Dounaevsky, and E. Shoshan, "Xampling: Analog to digital at sub-Nyquist rates," *IET Circuits, Devices and Systems*, vol. 5, no. 1, pp. 8–20, Jan. 2011.

[8] E. J. Candès and M. B. Wakin, "An introduction to compressive sampling," *IEEE Signal Process. Mag.*, vol. 25, no. 2, pp. 21–30, Mar. 2008.

[9] M. Elad, *Sparse and Redundant Representations: From Theory to Applications in Signal and Image Processing*. Springer, 2010.

[10] M. Mishali, Y. Eldar, and A. Elron, "Xampling: Signal acquisition and processing in union of subspaces," *IEEE Trans. Signal Process.*, vol. 59, no. 10, pp. 4719 –4734, Oct. 2011.

[11] S. Cotter, B. Rao, K. Engan, and K. Kreutz-Delgado, "Sparse solutions to linear inverse problems with multiple measurement vectors," *IEEE Trans. Signal Process.*, vol. 53, no. 7, pp. 2477–2488, Jul. 2005.

[12] L. Trefethen and D. Bau, *Numerical linear algebra*. Philadelphia: Society for Industrial and Applied Mathematics, 1997.